

# Bottomonium spectrum in the relativistic flux tube model

Bing Chen<sup>1,\*</sup>, Ailin Zhang<sup>2,†</sup> and Jin He<sup>1,‡</sup>

<sup>1</sup>*School of Electrical and Electronic Engineering, Anhui Science and Technology University, Fengyang 233100, China*

<sup>2</sup>*Department of Physics, Shanghai University, Shanghai 200444, China*

(Dated: January 30, 2020)

The bottomonium spectrum is far from being established. The structures of higher vector states, including the  $\Upsilon(10580)$ ,  $\Upsilon(10860)$ , and  $\Upsilon(11020)$  states, are still in dispute. In addition, whether the  $\Upsilon(10750)$  signal which was recently observed by the Belle Collaboration is a normal  $b\bar{b}$  state or not should be examined. Faced with such a situation, we carried out a systematic investigation of the bottomonium spectrum in the scheme of the relativistic flux tube (RFT) model. A Chew-Frautschi like formula was derived analytically for the spin average mass of bottomonium states. We further incorporated the spin-dependent interactions and obtained a complete bottomonium spectrum. We found that the most established bottomonium states can be explained in the RFT scheme. The  $\Upsilon(10750)$ ,  $\Upsilon(10860)$ , and  $\Upsilon(11020)$  could be predominantly the  $3^3D_1$ ,  $5^3S_1$ , and  $4^3D_1$  states, respectively. Our predicted masses of  $1F$  and  $1G$   $b\bar{b}$  states are in agreement with the results given by the method of lattice QCD, which can be tested by experiments in future. We also compared the RFT model with the quark potential model in detail. The differences of these two kinds of models were discussed.

PACS numbers: 12.39.-x, 12.40.Yx

## I. INTRODUCTION

The toponium system ( $t\bar{t}$ ) can hardly exist in nature due to the very short lifetime of the top quark ( $\approx 0.5 \times 10^{-24}$ s) [1]. Then the bottomonium is the heaviest meson system which has been researched by experiments for many years. This fact makes the bottomonium family occupy an important position in the hadron zoo and play a special role in the study of the strong interactions. A prominent feature of the bottomonium spectrum is that many excited states are below the threshold  $B\bar{B}$ , which provides a good platform to test the different kinds of effective theories and phenomenological models.

Comparing with the theoretical expectations, however, the complete bottomonium spectrum is far from being established. The first three bottomonium states, namely  $\Upsilon(1S)$ ,  $\Upsilon(2S)$ , and  $\Upsilon(3S)$ , were observed by the E288 Collaboration at Fermilab in 1977 [2, 3]. Since then nearly twenty bottomonium states have been established [4]. The experimental history of the  $b\bar{b}$  states has been reviewed in Ref. [5]. Here, we just briefly review some important measurements of bottomonium in the past fifteen years.

As shown in Fig. 1, after the discovery of  $\Upsilon(4S)$ ,  $\Upsilon(10860)$ , and  $\Upsilon(11020)$  states [6, 7], no progress had been made in searching for the excited  $b\bar{b}$  states for a long time until the CLEO Collaboration observed a  $1^3D_2$  candidate in the cascade process,  $\Upsilon(3S) \rightarrow \gamma\chi_b(2P) \rightarrow \gamma\gamma\Upsilon(1^3D_2) \rightarrow \gamma\gamma\chi_b(1P) \rightarrow \gamma\gamma\gamma\Upsilon(1S)$ , in 2004 [8]. This  $1D$  state was later confirmed by *BABAR* through the  $\Upsilon(1^3D_2) \rightarrow \pi^+\pi^-\Upsilon(1S)$  decay mode [9]. Furthermore, the *BABAR* sample may contain the  $\Upsilon(1^3D_1)$  and  $\Upsilon(1^3D_3)$  events though the significances of these two states were very low [9].

The spin singlet states of  $S$ - and  $P$ -wave  $b\bar{b}$  mesons, i.e.,

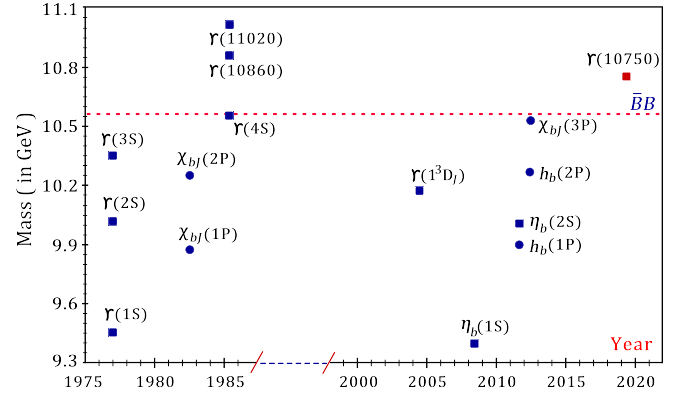


FIG. 1: The bottomonium states and their observed years.

$\eta_b(1S)$ ,  $\eta_b(2S)$ ,  $h_b(1P)$ , and  $h_b(2P)$ , have also been found by experiments in recent years. As a long-sought state, the  $\eta_b(1S)$  state was first observed by *BABAR* in the decay channel  $\Upsilon(3S) \rightarrow \gamma\eta_b(1S)$  [10], and subsequently confirmed in the decay channel  $\Upsilon(2S) \rightarrow \gamma\eta_b(1S)$  [11]. The  $\eta_b(1S)$  has also been observed by the CLEO Collaboration in the channel  $\Upsilon(3S) \rightarrow \gamma\eta_b(1S)$  [12], and by the Belle Collaboration in the channels  $h_b(nP) \rightarrow \gamma\eta_b(1S)$  ( $n = 1$  and  $2$ ) [13, 14].

The first probable signal of the  $\eta_b(2S)$  state was detected by the *BABAR* Collaboration [15] although their result was largely inconclusive. A clear evidence of  $\eta_b(2S)$  was achieved by the Belle Collaboration in the processes  $e^+e^- \rightarrow \Upsilon(5S) \rightarrow h_b(2P)\pi^+\pi^- \rightarrow \gamma\eta_b(2S)\pi^+\pi^-$  [13]. There the mass of  $\eta_b(2S)$  was measured by Belle as  $9999.0 \pm 3.5^{+2.8}_{-1.9}$  MeV.<sup>1</sup>

\*Electronic address: chenbing@ahstu.edu.cn

†Electronic address: zhangal@shu.edu.cn

‡Electronic address: hejin@ahstu.edu.cn

<sup>1</sup> Dobbs *et al.* analyzed  $(9.32 \pm 0.19) \times 10^6$   $\Upsilon(2S)$  recorded with the CLEO III detector and announced the observation of  $\eta_b(2S)$  in the reaction  $\Upsilon(2S) \rightarrow \gamma\eta_b(2S)$  [16]. However, their result was not confirmed by Belle with a larger sample of  $\Upsilon(2S)$  decays [17].

TABLE I: The measured mass and the observed decay mode for the  $\chi_{b(J)}(3P)$  state by the different collaborations.

State	Mass (MeV)	Decay mode	Collaboration
$\chi_{bJ}(3P)$	$10530 \pm 5 \pm 9$	$\Upsilon(1S)\gamma, \Upsilon(2S)\gamma$	ATLAS [21]
$\chi_{bJ}(3P)$	$10551 \pm 14 \pm 17$	$\Upsilon(1S)\gamma$	D0 [22]
$\chi_{b1}(3P)$	$10515.7^{+2.2+1.5}_{-3.9-2.1}$	$\Upsilon(1S)\gamma, \Upsilon(2S)\gamma,$	LHCb [23]
$\chi_{b1}(3P)$	$10511.3 \pm 1.7 \pm 2.5$	$\Upsilon(3S)\gamma$	LHCb [24]

The first evidence of spin-singlet state  $h_b(1P)$  was reported by *BABAR* in the sequential decays  $\Upsilon(3S) \rightarrow \pi^0 h_b(1P) \rightarrow \pi^0 \gamma \eta_b(1S)$  [18]. There the mass value of  $h_b(1P)$  was measured as  $9902 \pm 4 \pm 1$  MeV though the effective signal significance was only  $3.0 \sigma$ . The significant signal of  $h_b(1P)$  was achieved by Belle [13, 19] in the  $\pi^+ \pi^-$  missing spectrum of the reaction  $e^+ e^- \rightarrow \Upsilon(5S) \rightarrow h_b(1P) \pi^+ \pi^-$ . Meanwhile, the radial excited  $h_b(2P)$  was also observed in these measurements.<sup>2</sup> The  $h_b(1P)$  state was also found in the transition  $\Upsilon(4S) \rightarrow \eta h_b(1P)$  [14].

A  $\chi_b(3P)$  state was first discovered by the ATLAS Collaboration in the radiative decay modes of  $\chi_b(3P) \rightarrow \Upsilon(1S, 2S)\gamma$  [21], and subsequently confirmed by the D0 [22] and LHCb Collaborations [23, 24]. However, their measured masses were a little different from each other (see Table I).

Very recently, the Belle Collaboration discovered a new candidate of the upsilon resonance in the shape of cross sections of  $e^+ e^- \rightarrow \Upsilon(nS) \pi^+ \pi^-$  ( $n = 1, 2, 3$ ) [25]. Belle denoted this state as the  $\Upsilon(10750)$  and determined the mass and width as

$$M = 10752.7 \pm 5.9^{+0.7}_{-1.1} \text{ MeV}, \quad \Gamma = 35.5^{+17.6+3.9}_{-11.3-3.3} \text{ MeV}, \quad (1)$$

respectively, by the Breit-Wigner parametrization. Surely, more experimental confirmations are required for the  $\Upsilon(10750)$  state.

Obviously, it is not an easy task to establish the bottomonium spectrum completely because even many  $b\bar{b}$  states below the  $B\bar{B}$  threshold have not been discovered. However, the situation may be changed especially because of the running of Belle II [26]. It is expected that more excited bottomonium states will be detected in the near future. So it is time to investigate the spectrum of  $b\bar{b}$  by different approaches which incorporate the spirit of QCD.

So far, different types of quark potential model have been applied in studying the bottomonium spectrum, including the nonrelativistic [5, 27–30], the semirelativistic [31, 32], the relativized [33–35], and the relativistic [36, 37] versions. The bottomonium spectrum has also been studied by the Bethe-Salpeter equation [38], the coupled channel model [39–42], the QCD sum rule [43, 44], the Regge phenomenology [45–

<sup>2</sup> Belle also measured  $R \equiv \frac{\sigma(h_b(np)\pi^+\pi^-)}{\sigma(\Upsilon(2S)\pi^+\pi^-)}$  ( $n = 1, 2$ ) and the result indicated that the  $\Upsilon(5S) \rightarrow h_b(np)\pi^+\pi^-$  and  $\Upsilon(5S) \rightarrow \Upsilon(2S)\pi^+\pi^-$  processes have similar production ratios [19]. This interesting result not only implied the complicated structure of high excited  $\Upsilon$  states [20], but also provided a new route to search the unknown  $b\bar{b}$  states.

[48], the lattice QCD [49–51], and the method of perturbative QCD [52].

In this work, we will explore bottomonium spectrum in the scheme of the RFT model which can be rigorously derived from the Wilson area law in QCD [53]. The investigation of  $b\bar{b}$  spectrum here by the RFT model could be regraded as an extension of our previous work [54]. There we have shown that the RFT model can describe the masses of single heavy baryons well. Especially, the predicted masses of  $1D \Lambda_c^+$  and  $\Lambda_b^0$  states in Ref. [54] are in good agreement with the later measurements by the LHCb Collaboration [55, 56].

The manuscript is organized as follows. The RFT model is introduced in Sec. II where a spin average mass formula of the heavy quarkonia is derived. In Sec. III, we test the mass formula by the well measured  $b\bar{b}$  states. In Sec. IV, the spin-dependent interactions are incorporated and the complete bottomonium spectrum is presented. In Sec. V, we give further discussions about the differences of the RFT model and the quark potential model. Finally, the paper ends with the conclusion and summary.

## II. SPIN AVERAGE MASS FORMULA OF THE HEAVY QUARKONIA IN THE RFT MODEL

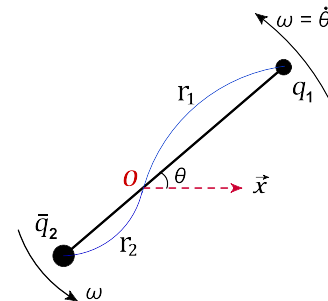


FIG. 2: Meson  $q_1 \bar{q}_2$  system in the RFT model.

The basic assumption of the RFT model is that the gluon field connecting the largely separated quarks in the QCD dynamical ground state could be regarded as a rigid straight tube-like color flux configuration [57]. Thus the angular momentum of the gluon field is taken into account by the RFT model, which is qualitatively different from the usual quark potential models. The authors of Refs. [58, 59] have shown that the RFT model can be derived from the Nambu-Goto QCD string model [60–62]. Furthermore, different aspects of the RFT model were investigated by different groups [63–70]. The deep relationship between the RFT model and QCD has also been verified in Refs. [53, 71]. The RFT model has been applied to study the masses of heavy-light mesons [72–74], charmonium states [75], single heavy baryons [54, 76], glueballs [77, 78], and other exotic hadrons [79].

As shown in Fig. 2, the Lagrangian of a  $q_1 \bar{q}_2$  meson in the

RFT model is written as [80]

$$\mathcal{L}(r_i, \dot{\theta}) = - \sum_{i=1}^2 \left[ m_i \sqrt{1 - (r_i \dot{\theta})^2} + \int_0^{r_i} \tau \sqrt{1 - (\rho \dot{\theta})^2} d\rho \right], \quad (2)$$

where  $m_i$  and  $r_i$  denote the mass of  $i$  ( $i = 1, 2$ ) quark and its distance from the center of gravity (see Fig. 2).  $\tau$  represents the string (flux tube) tension. Here, we only consider the transverse velocity of the quark and antiquark, i.e.,  $\dot{r}_i = 0$ . Then the total orbital angular momentum  $L$  is defined by

$$L = \frac{\partial \mathcal{L}}{\partial \dot{\theta}} = \sum_{i=1}^2 \left[ \frac{m_i r_i^2 \dot{\theta}}{\sqrt{1 - (r_i \dot{\theta})^2}} + \int_0^{r_i} \frac{\tau \rho^2 \dot{\theta}}{\sqrt{1 - (\rho \dot{\theta})^2}} d\rho \right]. \quad (3)$$

The Hamiltonian of  $q_1 \bar{q}_2$  meson is given by

$$H = \dot{\theta} L - \mathcal{L} = \sum_{i=1}^2 \left[ \frac{m_i}{\sqrt{1 - (r_i \dot{\theta})^2}} + \int_0^{r_i} \frac{\tau}{\sqrt{1 - (\rho \dot{\theta})^2}} d\rho \right]. \quad (4)$$

When we denote the velocity of the  $i$  quark which is attached with the flux tube as  $u_i = r_i \dot{\theta} = r_i \omega$ , the energy and orbital angular momentum can be written as

$$\epsilon = \sum_{i=1}^2 \left[ \frac{m_i}{\sqrt{1 - u_i^2}} + \frac{\tau}{\omega} \int_0^{u_i} \frac{dv}{\sqrt{1 - v^2}} \right], \quad (5)$$

and

$$L = \sum_{i=1}^2 \left[ \frac{m_i u_i^2}{\omega \sqrt{1 - u_i^2}} + \frac{\tau}{\omega^2} \int_0^{u_i} \frac{v^2 dv}{\sqrt{1 - v^2}} \right]. \quad (6)$$

We have set  $c = 1$  in natural units for simplicity. Eqs. (5) and (6) have also been obtained by the Wilson area law [53]. With Equations. (5) and (6), a mass formula for the heavy-light hadrons has been derived analytically in our previous work [54]. For the bottomonium system, the masses of  $b$  and  $\bar{b}$  quarks are denoted as  $m$ . Then Eqs. (5) and (6) become as

$$\epsilon = \frac{2m}{\sqrt{1 - u^2}} + \frac{2\tau}{\omega} \arcsin u, \quad (7)$$

and

$$L = \frac{2mu^2}{\omega \sqrt{1 - u^2}} + \frac{\tau}{\omega^2} (\arcsin u - u \sqrt{1 - u^2}). \quad (8)$$

Combining with the following relationship in the RFT model,

$$\frac{\tau}{\omega} = \frac{mu}{1 - u^2}, \quad (9)$$

we have

$$\epsilon = \frac{2m}{\sqrt{1 - u^2}} + \frac{2mu}{1 - u^2} \arcsin u, \quad (10)$$

and

$$\tau L = \frac{2m^2 u^3}{(1 - u^2)^{3/2}} + \frac{m^2 u^2}{(1 - u^2)^2} (\arcsin u - u \sqrt{1 - u^2}). \quad (11)$$

Since Eqs. (7) and (8) can be derived from the QCD [53], the  $m$  in the above equations could be regarded as the ‘‘current quark masses’’ of the bottom quark. In practice, the constituent quark mass is more suitable for the phenomenological analysis. To this end, we assume

$$m_b = \frac{m}{\sqrt{1 - u^2}}. \quad (12)$$

From Eqs. (7)–(11), we have

$$\epsilon = 2m_b (1 + f_1(u)); \quad \tau L = 2m_b^2 f_2(u). \quad (13)$$

In the above equations, we set the following functions,

$$f_1(u) = \frac{u}{\sqrt{1 - u^2}} \arcsin u, \quad (14)$$

and

$$f_2(u) = \frac{u^3}{\sqrt{1 - u^2}} + \frac{u^2}{2(1 - u^2)} (\arcsin u - u \sqrt{1 - u^2}). \quad (15)$$

Since  $m_b$  has included the relativistic effect, we may treat it as the constituent quark mass of the  $b$  quark. The treatment of  $m_b$  which includes the relativistic effect is different from the work [75] where the RFT model has been applied to investigate the assignment of  $X(3872)$ . As shown later, the velocity of bottom quark in the  $b\bar{b}$  meson is no more than  $0.50c$ . Then Eqs. (13) can be expanded as

$$\begin{aligned} \frac{\epsilon - 2m_b}{2m_b} &= f_1(u) \approx u^2 + O(u^4) + \dots, \\ \frac{\tau L}{2m_b^2} &= f_2(u) \approx u^3 + O(u^5) + \dots. \end{aligned} \quad (16)$$

If we ignore the higher order of  $u$ , the following relationship can be obtained:

$$\epsilon_L = 2m_b + \left( \frac{2}{m_b} \right)^{1/3} (\tau L)^{2/3}. \quad (17)$$

However, the validity of Eq. (17) is independent of the expansion method in Eqs. (16) since the relationship  $(f_1(u))^{1/2} \approx (f_2(u))^{1/3}$  always holds when the velocity of the bottom quark is taken from  $0.0c$  to  $0.9c$ . To illustrate this point, the variation of ratio  $(f_1(u))^{1/2} / (f_2(u))^{1/3}$  with the velocity of  $b$  quark in the bottomonium system is presented in Fig. 3.

In the following, we replace the string tension  $\tau$  by the parameter  $\sigma$  with the relationship  $\sigma \equiv 2\pi\tau$ . As done in Ref. [54], we further extend Eq. (17) to include the radial excited  $b\bar{b}$  states,

$$\epsilon_{nL} = 2m_b + \left( \frac{\sigma^2}{2\pi^2 m_b} \right)^{1/3} (\lambda n + L)^{2/3}. \quad (18)$$

This is a Chew-Frautschi like formula of the mass of  $b\bar{b}$  states. In our calculation, the mass of  $b$  quark  $m_b$ , the string tension parameter  $\sigma$ , and the dimensionless coefficient  $\lambda$  in Eq. (18) are determined directly by the well established  $1S$ ,  $1P$ , and  $2S$   $b\bar{b}$  states (see Sec. III for details). When the distance

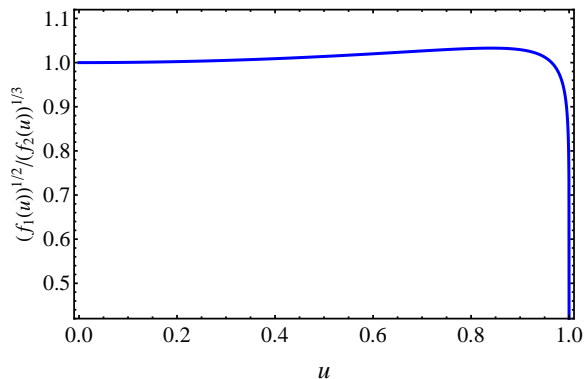


FIG. 3: The variation of ratio  $(f_1(u))^{1/2} / (f_2(u))^{1/3}$  with the velocity of bottom quark  $u$  in the bottomonium system.

between the  $b$  and  $\bar{b}$  quarks in a  $b\bar{b}$  meson is denoted as  $r$ , we have the relationship  $r = 2u/\omega$ . Combing with Eq. (9), we get

$$r = \frac{4\pi m_b}{\sigma} \frac{u^2}{\sqrt{1-u^2}}. \quad (19)$$

In the region of  $u \in 0.3c \sim 0.6c$ , we find  $u^2/\sqrt{1-u^2} \approx (0.95 \pm 0.02) \times f_1(u)$ . With Eqs. (13) and (18), we obtain the expression of  $r$  as

$$r = \left( \frac{10.8}{\sigma m_b} \right)^{1/3} (\lambda n + L)^{2/3}. \quad (20)$$

In next Section, we test the Eq. (18) by the measured masses of  $b\bar{b}$  states. In Sec. IV, we will incorporate the spin-dependent interactions and present a complete bottomonium spectrum.

### III. TESTING EQ. (18) BY THE MEASURED MASSES OF BOTTOMONIUM STATES

Three parameters in Eq. (18), namely the mass of bottom quark  $m_b$ , the string tension  $\sigma$ , and the dimensionless  $\lambda$ , should be fixed by the experimental data. We used the spin average masses of the  $1S$ ,  $2S$ , and  $1P$   $b\bar{b}$  states to fix the  $m_b$ ,  $\sigma$ , and  $\lambda$ . The spin average mass of  $1S$   $b\bar{b}$  is

$$\bar{M}(1S) = \frac{9398.7 + 9460.3 \times 3}{4} = 9444.9 \text{ MeV}, \quad (21)$$

and the average mass of  $2S$   $b\bar{b}$  is

$$\bar{M}(2S) = \frac{9999 + 10023.3 \times 3}{4} = 10017.2 \text{ MeV}. \quad (22)$$

Here, the masses of  $1S$  and  $2S$   $b\bar{b}$  states are taken from the latest ‘‘review of particle physics’’ (RPP) [4] by the Particle Data Group (PDG). Since the average mass of  $1^3P_0$ ,  $1^3P_1$ , and  $1^3P_2$   $b\bar{b}$  states is quite close to the  $1^1P_1$  state (see Ref. [81] for more discussions), we take the mass of  $h_b(1P)$  as the average

mass of  $1P$   $b\bar{b}$  states. Specifically, the world average mass of  $h_b(1P)$  state, i.e., 9899.3 MeV [4], is used to fix the parameters in Eq. (18). With the masses of  $\bar{M}(1S)$ ,  $\bar{M}(2S)$ , and  $h_b(1P)$ , the parameters are fixed as

$$m_b = 4.7224 \text{ GeV}, \quad \sigma = 2.96 \text{ GeV}^2, \quad \lambda = 1.41. \quad (23)$$

Here, the mass of the  $b$  quark which was fixed by Eq. (18) is larger than its one-loop pole mass, i.e.,  $m_{b,1\text{-loop}} = 4.550$  GeV [48]. Furthermore, the velocity of the  $b$  quark could be estimated to be  $0.46 \pm 0.01 c$  by comparing the value of  $m_b$  with the current mass of the  $b$  quark, i.e.,  $4.18_{-0.02}^{+0.03}$  GeV [4].

With the values of  $m_b$ ,  $\sigma$ , and  $\lambda$ , the center of gravity of the other  $n^{2S+1}L_J$  multiplet can be calculated directly. At present, the masses of  $\Upsilon(3S)$ ,  $h_b(2P)$  and  $\Upsilon_2(1D)$  states have been well measured by different experiments [4]. A comparison of the masses of these  $b\bar{b}$  states with the predictions by Eq. (18) is given in the Table II.

TABLE II: The predicted spin average masses of the  $1D$ ,  $2P$ , and  $3S$   $b\bar{b}$  multiplets (in MeV). The measured masses of observed candidates [4] are also listed for comparison.

$nL$	State	Measured mass	Prediction
$1D$	$\Upsilon_2(1D)$	$10163.7 \pm 1.4$	10166
$2P$	$h_b(2P)$	$10259.8 \pm 1.2$	10262
$3S$	$\Upsilon(3S)$	$10355.2 \pm 0.5$	10352

The mass of  $h_b(2P)$  is predicted to be 10262 MeV which is consistent with the experimental result. The  $\eta_b(3S)$  state has not been discovered by the experiment. Nevertheless, the spin average mass of the  $2S$  bottomonium states is about 6 MeV below the  $\Upsilon(2S)$  state [see Eq. (22)]. So one could reasonably expect the average mass of  $3S$  states to be about 10350 MeV, which is also close to our prediction. As argued in Ref. [15], two  $D$ -wave  $b\bar{b}$  states, namely the  $\Upsilon(10152)$  and  $\Upsilon_3(10173)$ , may have been detected in the experimental data by the CLEO [8] and BABAR [9] collaborations. Although the measured masses of these two states need more confirmation, the average mass of the  $\Upsilon(10152)$ ,  $\Upsilon_2(10164)$ , and  $\Upsilon_3(10173)$  states

$$\frac{10152 \times 3 + 10163.7 \times 5 + 10173 \times 7}{15} = 10165.7 \text{ MeV} \quad (24)$$

is quite consistent with our result (see Table II).

As shown above, the predicted average masses of  $\Upsilon(3S)$ ,  $h_b(2P)$ , and  $\Upsilon_2(1D)$  multiplets are well comparable with the experimental results. For completeness, we incorporate the spin-dependent interactions and give a whole bottomonium spectrum in the next section.

#### IV. THE COMPLETE BOTTOMONIUM SPECTRUM BY INCORPORATING THE SPIN-DEPENDENT INTERACTIONS

For simplicity, we consider the color hyperfine interaction

$$H_{\text{hyp}} = \frac{4\alpha_s}{3m_b^2} \left( \frac{8\pi}{3} \delta^3(\mathbf{r}) \mathbf{s}_b \cdot \mathbf{s}_{\bar{b}} + \frac{1}{r^3} \hat{S}_{b\bar{b}} \right), \quad (25)$$

which arises from the one gluon exchange (OGE) forces, and the following spin-orbit term

$$H_{\text{so}} = \frac{1}{m_b^2} \left( \frac{2\alpha_s}{r^3} - \frac{b}{2r} \right) \mathbf{S} \cdot \mathbf{L}, \quad (26)$$

which includes the OGE spin orbit and the longer-ranged inverted spin-orbit terms. This type of spin-dependent interactions has been applied to investigate the mass spectrum of charmonia states [82]. The  $\hat{S}_{b\bar{b}}$  denotes the tensor operator. The “ $\delta^3(\mathbf{r})$ ” function which comes from a contact hyperfine interaction can be simulated by different forms of smearing functions [33, 83]. In our calculations, we take the following smearing function,

$$f(\mathbf{r}) = \frac{4}{\pi^2 r_0^2} \frac{e^{-\sqrt{r/r_0}}}{r}, \quad (27)$$

to reproduce the mass splitting of  $nS$  ( $n \geq 2$ ).<sup>3</sup> Here, we take the  $r_0$  as  $0.94 \text{ GeV}^{-1}$ . Because of the heavy masses, the distance between  $b$  and  $\bar{b}$  quarks in the low-lying bottomonium states is much smaller. Therefore, one should treat the running coupling constant  $\alpha_s$  in Eqs. (25) and (26) seriously. We use the following,

$$\alpha_s(r) = \alpha_0 \text{Erf} \left[ \left( \frac{m_b r}{0.72\pi^2} \right)^{5/2} \right], \quad (28)$$

to simulate the running coupling constant, where the  $\text{Erf}[\dots]$  refers to the error function. In our calculations, the running coupling constant is assumed to saturate at 0.68, i.e.,  $\alpha_0 = 0.68$ . To reduce the free parameters, we take the value of  $b$  in Eq. (26) as the string tension  $\tau$  in the RFT model, i.e.,  $b = \sigma/2\pi = 0.471 \text{ GeV}^2$ . With Eqs. (20), (25), (27), and (28), the splitting masses of  $n^3S_1$  and  $n^1S_0$  states ( $n \geq 2$ ) are presented in Table III.

TABLE III: The mass splitting of  $n^3S_1$  and  $n^1S_0$  states (in MeV).

$\Delta M(nS)$	$n = 2$	$n = 3$	$n = 4$	$n = 5$	$n = 6$
Our	23.9	20.7	13.2	9.3	7.0
Ref. [34]	27	18	12	9	5
Ref. [27]	25	17	13	11	9

<sup>3</sup> The distance of  $b$  and  $\bar{b}$  quarks in the  $1S$  state is given as 0 by Eq. (20), which is obviously underestimated. So we do not reproduce the mass splitting of the  $1^3S_1$  and  $1^1S_0$   $b\bar{b}$  states.

Obviously, our results in Table III are comparable with those from Refs. [27, 34]. As shown later, the masses of most known  $b\bar{b}$  states can also be reproduced, though our method is quite phenomenological.

#### A. $nS$ ( $n \geq 2$ ) states

With the predicted splitting masses in Table III, the masses of  $n^1S_0$  and  $n^3S_1$  bottomonium states ( $n \geq 2$ ) are predicted in Table IV where the experimental data [4] and the results from other works [29, 34, 41] are also listed for comparison.

TABLE IV: The masses of the  $nS$  ( $n \geq 2$ )  $b\bar{b}$  states (in MeV).

States	Expt. [4]	Our	Ref. [34]	Ref. [29]	Ref. [41]
$0^{+}(2S)$	9999±4	9999	9976	9955	10005
$1^{--}(2S)$	10023.3±0.3	10023	10003	9979	10026
$0^{+}(3S)$		10337	10336	10338	10338
$1^{--}(3S)$	10355.2±0.5	10357	10354	10359	10352
$0^{+}(4S)$		10627	10623	10663	10593
$1^{--}(4S)$	10579.4±1.2	10637	10635	10683	10603
$0^{+}(5S)$		10878	10869	10956	10813
$1^{--}(5S)$	10889.9 <sup>+3.2</sup> <sub>-2.6</sub>	10887	10878	10975	10820
$0^{+}(6S)$		11111	11097	11226	11008
$1^{--}(6S)$	10992.9 <sup>+10.0</sup> <sub>-3.1</sub>	11118	11102	11243	11023

As shown in Table IV, the masses of well measured  $\eta_b(2S)$ ,  $\Upsilon(2S)$ , and  $\Upsilon(3S)$  states are reproduced in our scheme. The predicted mass of the unknown  $\eta_b(3S)$  state is 10337 MeV which is comparable with these results from Refs. [29, 34, 41].

The masses of the  $\Upsilon(4S)$ ,  $\Upsilon(5S)$ , and  $\Upsilon(6S)$  obtained by the RFT model are quite close to the results given by the Godfrey-Isgur model [34]. Our results favor the  $\Upsilon(10860)$  as a predominantly  $5^3S_1$  state. Interestingly, a recent work based on the lattice QCD also suggested the  $\Upsilon(10860)$  as a  $5^3S_1$  state [84]. The mass of  $\Upsilon(4S)$  predicted by the RFT model is about 60 MeV higher than the measured mass of  $\Upsilon(10580)$  (see Table IV). The mass of the  $\Upsilon(4S)$  state predicted in Refs. [5, 27–29, 34, 41] was also larger than the  $\Upsilon(10580)$  state. In the quark potential models, the mass gap between the  $3^3S_1$  and  $4^3S_1$   $b\bar{b}$  states is expected to be larger than the gap between the  $4^3S_1$  and  $5^3S_1$  states. However, the experimental measurement is contrary to the expectation, i.e.,

$$\Delta M(\Upsilon(10580) - \Upsilon(10355)) \approx 224.2 \text{ MeV}, \quad (29)$$

which is smaller than

$$\Delta M(\Upsilon(10860) - \Upsilon(10580)) \approx 310.5 \text{ MeV}. \quad (30)$$

It indicates that the mass of  $\Upsilon(4S)$  shifts down about 40~50 MeV due to a particular mechanism. This anomalously mass gap of “ $\Upsilon(4S) - \Upsilon(3S)$ ” and “ $\Upsilon(5S) - \Upsilon(4S)$ ” cannot simply be solved by the naïve quark model. Törnqvist proposed a solution to this puzzle. Specifically, it may be disentangled by considering the coupled-channel effects [40]. More importantly, the masses of  $\Upsilon(5S)$  and  $\Upsilon(6S)$  were well predicted in

the scheme of the coupled-channel model [40] before the observations of candidates, i.e.,  $\Upsilon(10860)$  and  $\Upsilon(11020)$  [6, 7]. The scheme suggested by Törnqvist was supported by the recent work [42].

If the  $\Upsilon(11020)$  is a pure  $6^3S_1$   $b\bar{b}$  state, its measured mass is about 100~200 MeV lower than the prediction by the RFT model and other methods [29, 34, 41, 85]. So it seems that the  $\Upsilon(11020)$  is not a pure  $6S$  upsilon resonance. This conclusion is partially supported by the analysis of its dielectron widths [85] (see Sec. IV C).

### B. $nP$ states

The masses of  $nP$  ( $n = 1 \sim 5$ )  $b\bar{b}$  states which are predicted by the RFT model are listed in Table V with the experimental data [4] and other theoretical results from Refs. [29, 34, 36]. Up to now, the  $1P$  and  $2P$  bottomonium states have been well established [4]. Obviously, the masses of these states are well reproduced by the RFT model.

TABLE V: The masses of the  $nP$   $b\bar{b}$  states (in MeV).

States	Expt. [4]	Our	Ref. [34]	Ref. [36]	Ref. [29]
$0^{++}(1P)$	9859.4±0.7	9854	9847	9859	9806
$1^{++}(1P)$	9892.8±0.6	9893	9876	9892	9819
$1^{+-}(1P)$	9899.3±0.8	9899	9882	9900	9821
$2^{++}(1P)$	9912.2±0.6	9911	9897	9912	9825
$0^{++}(2P)$	10232.5±0.9	10239	10226	10233	10205
$1^{++}(2P)$	10255.5±0.7	10259	10246	10255	10217
$1^{+-}(2P)$	10259.8±1.2	10262	10250	10260	10220
$2^{++}(2P)$	10268.7±0.7	10268	10261	10268	10224
$0^{++}(3P)$		10551	10522	10521	10540
$1^{++}(3P)$	10513.4±0.7	10557	10538	10541	10553
$1^{+-}(3P)$		10556	10541	10544	10556
$2^{++}(3P)$	10524.0±0.8	10556	10550	10550	10560
$0^{++}(4P)$		10815	10775	10781	10840
$1^{++}(4P)$		10817	10788	10802	10853
$1^{+-}(4P)$		10815	10790	10804	10855
$2^{++}(4P)$		10814	10798	10812	10860
$0^{++}(5P)$		11053	11004	...	11115
$1^{++}(5P)$		11053	11014	...	11127
$1^{+-}(5P)$		11051	11016	...	11130
$2^{++}(5P)$		11049	11022	...	11135

The candidates of  $3P$  bottomonium states have been detected by the ATLAS [21], D0 [22], and LHCb [23, 24] collaborations (see Table I). The masses of the  $\chi_{b1}(3P)$  and  $\chi_{b2}(3P)$  collected by the PDG are listed in Table V. The experimental results are about 20~40 MeV smaller than the theoretical results. One notices that the predicted masses  $3P$   $b\bar{b}$  states are about 30~100 MeV above the thresholds of  $B\bar{B}$ ,  $B\bar{B}^* + B^*\bar{B}$ , and  $B^*\bar{B}^*$  decay channels. So the coupled-channel effect may affect the properties of  $3P$  bottomonium states in-

cluding their masses.<sup>4</sup> More theoretical and experimental efforts are desirable for the  $3P$   $b\bar{b}$  states in future.

The  $4P$  and  $5P$  bottomonium states are predicted around 10800 and 11050 MeV, respectively, which means these states locate above the open-bottom thresholds. Then the Okubo-Zweig-Iizuka allowed decays are probable for these states. In Ref. [34], the investigation of strong decays by the  $^3P_0$  model indicated that the  $\chi_{b0}(4P)$  state mainly decays through the  $B\bar{B}$  and  $B^*\bar{B}^*$  channels while the  $B\bar{B}^* + B^*\bar{B}$  is the largest decay channel for the  $\chi_{b1}(4P)$ ,  $\chi_{b2}(4P)$ , and  $h_b(4P)$  states. Different from the  $4P$  bottomonium states, the largest decay channel of  $5P$  states is the  $B^*\bar{B}^*$ . The total decay widths of  $4P$  and  $5P$  bottomonium states were predicted to be 30~70 MeV. The decays predicted in Ref. [35] were slightly different from these results in Ref. [34]. Of course, discovery of these high  $P$ -wave bottomonium states is a great challenge for present experiments.

### C. $nD$ states

So far only one  $D$ -wave  $b\bar{b}$  state, namely  $\Upsilon_2(1D)$ , was listed in the summary table of PDG [4]. Its measured mass, i.e.,  $10163.7 \pm 1.7$  MeV, is quite in agreement with our prediction (see Table VI). The visible evidence of the  $1^3D_1$  and  $1^3D_3$  bottomonium states at 10152 and 10173 MeV [8, 9], respectively, was pointed out in Ref. [15]. Our predictions in Table VI are comparable with these preliminary results. Our results are also consistent with the predicted masses of  $1D$   $b\bar{b}$  states by lattice QCD [49].

None of the  $2D$   $b\bar{b}$  states have been announced by any experiments. Nevertheless, Beveren and Rupp found the  $\Upsilon(2D)$  signal with 10.7 standard deviations [87] by reanalyzing the BABAR data [88]. There the mass of  $\Upsilon(2D)$  was fitted to be  $10495 \pm 5$  MeV, which is a bit larger than the predictions in Table VI.

As mentioned before, a  $1^{--}$  structure  $\Upsilon(10750)$  which was discovered by the Belle collaboration [25] is still unclear. Since the  $3^3D_1$   $b\bar{b}$  state is expected to have a mass around 10740 MeV, the  $\Upsilon(10750)$  could be a good  $3D$  candidate. Due to the significant mixing between the  $(n+1)^3S_1$  and  $n^3D_1$  states ( $n \geq 3$ ), the magnitude of dielectron widths of the mixed  $\tilde{\Upsilon}(n^3D_1)$  resonances ( $n = 3, 4, 5$ ) can increase by 2 orders [85]. For the  $\tilde{\Upsilon}(3D)$  state, the dielectron width was obtained to be  $0.095^{+0.028}_{-0.025}$  keV, which indicated that the predominantly  $3^3D_1$   $b\bar{b}$  state can be produced in the  $e^+e^-$  annihilation process with the high statistics data. Furthermore, the decay width of the  $3^3D_1$   $b\bar{b}$  state was obtained as 54.1 MeV [35] which is comparable with the measurement by the Belle Collaboration [25] [see Eq. (1)]. So the  $\Upsilon(10750)$  could be predominantly a  $3^3D_1$   $b\bar{b}$  state in our scheme. However, the other explanations suggested in Refs. [89, 90] are also possible for the  $\Upsilon(10750)$

<sup>4</sup> However, the practical calculations in Ref. [86] did not support this conjecture. There the  $\chi_b(3P)$  state was suggested to be the (almost) pure bottomonia.

state. For revealing the inner structure of  $\Upsilon(10750)$ , more precise measurements including the dielectron width and the branching ratios of  $\Gamma(B\bar{B}) : \Gamma(B\bar{B}^* + B^*\bar{B}) : \Gamma(B^*\bar{B}^*)$  are needed in future.

TABLE VI: The masses of the  $nD$   $b\bar{b}$  states (in MeV).

States	Expt. [4]	Our	Ref. [34]	Ref. [36]	Ref. [29]
$1^-(1D)$		10136	10138	10154	10074
$2^-(1D)$	$10163.7 \pm 1.7$	10164	10147	10161	10075
$2^+(1D)$		10167	10148	10163	10074
$3^-(1D)$		10183	10155	10166	10073
$1^-(2D)$		10467	10441	10435	10423
$2^-(2D)$		10476	10449	10443	10424
$2^+(2D)$		10475	10450	10445	10424
$3^-(2D)$		10478	10455	10449	10423
$1^-(3D)$	$10752.7 \pm 5.9^{+0.7}_{-1.1}$	10742	10698	10704	10731
$2^-(3D)$		10744	10705	10711	10733
$2^+(3D)$		10742	10706	10713	10733
$3^-(3D)$		10740	10711	10717	10733
$1^-(4D)$	$10992.9^{+10.0}_{-3.1}$	10987	10928	10949	11013
$2^-(4D)$		10986	10934	10957	11016
$2^+(4D)$		10984	10935	10959	11015
$3^-(4D)$		10981	10939	10963	11015

According to the predicted masses by the RFT model and other methods [29, 34, 36], the  $4D$   $b\bar{b}$  states should have the masses around 10950 MeV. The controversial  $\Upsilon(11020)$  state might have a significant  $4^3D_1$  component since its mass is quite close to the prediction of the  $4^3D_1$  state. Furthermore, the dielectron width of the pure  $6S$   $\Upsilon$  state was given about 0.274 KeV [85], which is about two times larger than the experimental measurement of  $\Upsilon(11020)$ . This result also indicated that the  $S$ - $D$  mixing effect should be significant for the  $\Upsilon(11020)$  state.

#### D. High orbital excited states

Up to now, none of the high orbital excited  $b\bar{b}$  mesons including  $F$ -,  $G$ -, and  $H$ -wave states have been announced by any experiments. Obviously, it is a challenge for experiments to discover these states. However, the situation may have changed while the SuperKEKB facility has ran last year [26]. With the event numbers about  $2 \times 10^6$   $\Upsilon(2^3D_1)$  states produced at Belle II in future, the observation of  $F$ -wave  $b\bar{b}$  state could be accessible [26].

The masses of the  $1F$   $b\bar{b}$  states are predicted in the region around 10400 MeV (see Table VII), which is comparable with the results given by the lattice nonrelativistic QCD [50]. The  $1G$   $b\bar{b}$  masses are predicted around 10590 MeV which are slightly above the  $B\bar{B}$  threshold at 10.56 GeV. Our predicted masses of  $1G$   $b\bar{b}$  states seem to be larger than the results given by the quark potential models [5, 34–36], but very close to the results from the lattice QCD [50], where the masses of  $4^{--}$

TABLE VII: The masses of high orbital excited  $b\bar{b}$  states (in MeV).

States	Our	Ref. [34]	Ref. [35]	Ref. [36]	Ref. [5]
$2^{++}(1F)$	10376	10350	10362	10343	10315
$3^{++}(1F)$	10391	10355	10366	10346	10321
$3^{+-}(1F)$	10391	10355	10366	10347	10322
$4^{++}(1F)$	10400	10358	10369	10349	...
$2^{++}(2F)$	10668	10615	10605	10610	10569
$3^{++}(2F)$	10670	10619	10609	10614	10573
$3^{+-}(2F)$	10668	10619	10609	10615	10573
$4^{++}(2F)$	10667	10622	10612	10617	...
$2^{++}(3F)$	10920	10850	10809	...	10782
$3^{++}(3F)$	10918	10853	10812	...	10785
$3^{+-}(3F)$	10916	10853	10812	...	10785
$4^{++}(3F)$	10912	10856	10815	...	...
$3^{--}(1G)$	10588	10529	10533	10511	10506
$4^{--}(1G)$	10592	10531	10535	10512	...
$4^{+-}(1G)$	10591	10530	10534	10513	...
$5^{--}(1G)$	10592	10532	10536	10514	...
$3^{--}(2G)$	10851	10769	10745	...	10712
$4^{--}(2G)$	10848	10770	10747	...	...
$4^{+-}(2G)$	10846	10770	10747	...	...
$5^{--}(2G)$	10842	10772	10748	...	...
$4^{++}(1H)$	10778	...	...	10670	...
$5^{++}(1H)$	10776	...	...	10671	...
$5^{+-}(1H)$	10774	...	...	10671	...
$6^{++}(1H)$	10769	...	...	10672	...

and  $4^{--}$   $b\bar{b}$  states were predicted as

$$\begin{aligned} M(^1G_4) &= 10581 \pm 17 \text{ MeV}, \\ M(^3G_4) &= 10587 \pm 18 \text{ MeV}. \end{aligned} \quad (31)$$

#### V. FURTHER DISCUSSIONS: A COMPARISON OF RESULTS GIVEN BY THE RFT MODEL AND THE QUARK POTENTIAL MODEL

From Tables IV–VI, one may notice that the masses predicted by the quark potential model [34–36] and the RFT model are quite similar for these low-lying  $b\bar{b}$  states. Since the higher excited bottomonium states have not been found by experiments, there is no criterion from the experimental measurements to distinguish these models. In this section, we give a comparison of the RFT model and the quark potential model.

From a phenomenological point of view, the confinement mechanism for the quarks in a hadron system could be mimicked in two simple ways. In the quark potential model, the confinement mechanism is usually implemented by a long-distance linear potential [91, 92]. Differently, a dynamical flux tube in the RFT model is responsible for the confinement mechanism [57, 63]. In the following, we compare these two models from three aspects.

First, we may compare the Hamiltonian of the RFT model to the relativized quark potential (RQP) model [33], directly. The following spinless Salpeter Hamiltonian of the RQP model

$$H^{\text{RQP}} = 2\sqrt{p^2 + m^2} + \sigma r, \quad (32)$$

has been used to calculate the mass spectra of bottomonium states in Ref. [34] where the Coulomb potential in short range and a mass-renormalized constant  $C$  were supplemented. For comparing with the Hamiltonian of Eq. (32), we rewrite the Hamiltonian of RFT model as

$$H^{\text{RFT}} = 2\sqrt{p^2 + m^2} + \frac{\sigma r}{2} \left( \frac{\arcsin \varepsilon_1}{\varepsilon_1} + \varepsilon_2 \right) + \frac{\sqrt{p_r^2 + m^2}}{16p_t^2} \varepsilon_2 \sigma^2 r^2 \left( \frac{\arcsin \varepsilon_1}{\varepsilon_1} - \varepsilon_2 \right)^2, \quad (33)$$

which was obtained by an expansion in the string tension  $\sigma$  [71]. The parameters  $\varepsilon_1$  and  $\varepsilon_2$  in Eq. (33) were defined as

$$\varepsilon_1 = \sqrt{\frac{p_t^2}{p^2 + m^2}}; \quad \varepsilon_2 = \sqrt{\frac{p_r^2 + m^2}{p^2 + m^2}}. \quad (34)$$

In Eqs. (33) and (34),  $p_r$ ,  $p_t$ , and  $p$  denote the radial, transverse, and total momentum of the quark which was attached with the flux tube in a meson system. If the mass of the quark  $q$  in a  $q\bar{q}$  meson tends to infinity (i.e.,  $m \rightarrow \infty$ ), we have the limits:  $\varepsilon_1 \rightarrow 0$  and  $\varepsilon_2 \rightarrow 1$ , since the  $p_r$ ,  $p_t$  and  $p$  are far smaller than the quark mass. In this limit, the flux tube model reduces to a quark model with linear confinement potential [58]. But the realistic mass of  $b$  quark in the bottomonium system is finite; the contribution of flux tube cannot reduce to a simple static potential [78].

Secondly, the following formula of excited energy which was obtained by the RFT model (also see Eq. (18) in Sec. II)

$$E_{nL}^{\text{RFT}} = \left( \frac{\sigma^2}{2\pi^2 m_b} \right)^{1/3} (1.41n + L)^{2/3}, \quad (35)$$

is also different from the result which was given by the quark potential model. In principle, the spinless Salpeter equation or the Schrödinger equation with linear confinement potential can hardly be solved analytically. But the Schrödinger equation with linear potential, i.e., the nonrelativistic version of Eq. (32), can be solved approximately by the perturbation expansion method [93], the Wentzel-Kramers-Brillouin approach [94], the variational method [95], and the shifted  $1/N$  expansion method [96]. By comparing with the numerical results in Refs. [95, 97], one may find that precision of the approximate solution obtained by the variational method [95] is best for the excited energy of meson systems. According to the results in Ref. [95], we could write the energy formula as

$$E_{nL}^{\text{var.}} = \left( \frac{6.645\sigma^2}{m_b} \right)^{1/3} (1.80n + L + 1.40)^{2/3}. \quad (36)$$

This is an approximate formula for the excited energy of low radial  $b\bar{b}$  excitations, which could be regarded as the approximate solution of the Schrödinger equation with linear confinement potential. Obviously, it is quite different from Eq. (35) which was deduced from the RFT model.

Finally, we may directly compare the spin average masses of  $b\bar{b}$  states, which were predicted by the RFT model, to the results given by a nonrelativistic constituent quark model [5]. The concrete results of the corresponding  $n^{2S+1}L_J$  multiplet with their differences are listed in Table VIII. Obviously, the differences of predicted masses given by two models are smaller than 50 MeV for these low excited  $b\bar{b}$  states, including  $3S$ ,  $4S$ ,  $2P$ ,  $3P$ , and  $1D$  states. However, the discrepancy of predictions becomes large for the higher excited bottomonium states. Especially for the high orbital excitations, the differences of predicted masses are very remarkable. This interesting result can be naturally explained since the flux tube can carry both angular momentum and energy. In fact, this point is conceptually different from the quark potential models [57].

TABLE VIII: A comparison of the spin average masses which were predicted by the RFT model and the nonrelativistic constituent quark model [5] (in MeV).

$n^{2S+1}L_J$	1S	2S	3S	4S	5S
Our	Input	Input	10352	10634	10885
Ref. [5]	9490	10009	10344	10607	10818
$\delta M$	...	...	8	27	67
$n^{2S+1}L_J$	1P	2P	3P	4P	5P
Our	Input	10262	10556	10815	11051
Ref. [5]	9879	10240	10516	10744	...
$\delta M$	-	22	40	71	...
$n^{2S+1}L_J$	1D	2D	3D	4D	5D
Our	10167	10475	10742	10984	11209
Ref. [5]	10123	10419	10658	10860	...
$\delta M$	44	56	84	124	...
$n^{2S+1}L_J$	1F	2F	3F	1G	2G
Our	10391	10668	10916	10591	10846
Ref. [5]	10322	10573	10785	10506	10712
$\delta M$	69	95	131	85	134

## VI. CONCLUSION AND SUMMARY

In this work, we derived a Chew-Frautschi like formula which can give an intuitive description of the spin average mass of the heavy quarkonium systems. With the measured masses of  $1S$ ,  $2S$ , and  $1P$   $b\bar{b}$  states, we fixed the three parameters in the Chew-Frautschi like formula, namely, the mass of  $b$  quark, string tension  $\sigma$ , and dimensionless parameter  $\lambda$ . Then we tested the mass formula by comparing the predicted spin average masses of  $3S$ ,  $2P$ , and  $1D$  states to the experimental results. The comparison implied that the Chew-Frautschi like formula could describe the spin average masses of high



excited  $b\bar{b}$  states well.

Inspired by a good description of the spin average mass, we further incorporate the spin-dependent interactions which include the OGE forces and the longer-ranged inverted spin-orbit term. As shown in the Tables IV and V, the measured masses of the  $nS$  ( $2 \leq n \leq 6$ ) and  $nP$  ( $n = 1$  and  $2$ ) states were well reproduced. The predicted masses of  $nD$  and other high bottomonium states in Tables VI and VII could be tested in future.

In addition, the differences between the RFT model and the quark potential model have also been discussed. To further reveal the role of the flux tube in the RFT model, we also compared the masses predicted by a nonrelativistic constituent quark model [5] and the RFT model. We list the main conclusions below.

- (1) The  $\Upsilon(10860)$  could be explained as a predominant  $5S$  state since its measured mass is very close to the predictions (see Table IV). The  $\Upsilon(10580)$  and  $\Upsilon(11020)$  cannot be regarded as the pure  $4S$  and  $6S$  states, respectively, since the predicted masses are much larger than the measurements.
- (2) The newly discovered  $\Upsilon(10750)$  could be regarded as a good candidate of the predominant  $3^3D_1$  state since the measured mass is in good agreement with our prediction.
- (3) The measured masses of  $3P$   $b\bar{b}$  states seem to be about 20–30 MeV smaller than the theoretical results.

- (4) Our predicted mass of the  $1^3D_2$   $b\bar{b}$  state is consistent with the experimental value. The predicted masses of  $1^3D_1$  and  $1^3D_3$  states are also comparable with the signals detected by the CLEO [8] and BABAR [9] collaborations.

In summary, the bottomonium spectrum has been systematically studied by the RFT model, which could be regarded as an important supplement to the available investigations of the bottomonium spectrum. Since the relativistic color flux tube carries both energy and momentum, the RFT model presents a different dynamics picture for the heavy quarkonia system. The larger predicted masses of the high orbital excited states by the RFT model can be tested by the experiments in future. Combining with our previous work [54], the RFT model has provided a reasonable scheme to describe the masses of single heavy baryons and heavy quarkonium. We may try to extend the RFT model to analyze the mass spectrum of light meson system in future.

### Acknowledgments

We thank Professor Xiang Liu for the helpful suggestions and A. Bondar for telling us the discovery history of the  $\eta_b(2S)$  state. This research was supported in part by the National Natural Science Foundation of China under Grants No. 11305003 and No. 11975146.

- 
- [1] I. I. Y. Bigi, Y. L. Dokshitzer, V. A. Khoze, J. H. Kuhn and P. M. Zerwas, Production and decay properties of ultraheavy quarks, *Phys. Lett. B* **181**, 157 (1986).
  - [2] S. W. Herb *et al.*, Observation of a Dimuon Resonance at 9.5 GeV in 400-GeV Proton-Nucleus Collisions, *Phys. Rev. Lett.* **39**, 252 (1977).
  - [3] W. R. Innes *et al.*, Observation of Structure in the  $\Upsilon$  Region, *Phys. Rev. Lett.* **39**, 1240 (1977), Erratum, *Phys. Rev. Lett.* **39**, 1640 (1977).
  - [4] M. Tanabashi *et al.* (Particle Data Group), Review of particle physics, *Phys. Rev. D* **98**, 030001 (2018).
  - [5] J. Segovia, P. G. Ortega, D. R. Entem and F. Fernández, Bottomonium spectrum revisited, *Phys. Rev. D* **93**, 074027 (2016).
  - [6] D. Besson *et al.* (CLEO Collaboration), Observation of New Structure in the  $e^+e^-$  Cross-Section above the  $\Upsilon(4S)$ , *Phys. Rev. Lett.* **54**, 381 (1985).
  - [7] D. M. J. Lovelock *et al.*, Masses, Widths, And Leptonic Widths of the Higher Upsilon Resonances, *Phys. Rev. Lett.* **54**, 377 (1985).
  - [8] G. Bonvicini *et al.* (CLEO Collaboration), First observation of a  $\Upsilon(1D)$  state, *Phys. Rev. D* **70**, 032001 (2004).
  - [9] P. del Amo Sanchez *et al.* (BABAR Collaboration), Observation of the  $\Upsilon(1^3D_J)$  bottomonium state through decays to  $\pi^+\pi^-\Upsilon(1S)$ , *Phys. Rev. D* **82**, 111102 (2010).
  - [10] B. Aubert *et al.* (BABAR Collaboration), Observation of the bottomonium ground state in the decay  $\Upsilon(3S) \rightarrow \gamma\eta_b$ , *Phys. Rev. Lett.* **101**, 071801 (2008), Erratum: [*Phys. Rev. Lett.* **102**, 029901 (2009)].
  - [11] B. Aubert *et al.* (BABAR Collaboration), Evidence for the  $\eta_b(1S)$  Meson in Radiative  $\Upsilon(2S)$  Decay, *Phys. Rev. Lett.* **103**, 161801 (2009).
  - [12] G. Bonvicini *et al.* (CLEO Collaboration), Measurement of the  $\eta_b(1S)$  mass and the branching fraction for  $\Upsilon(3S) \rightarrow \gamma\eta_b$ , *Phys. Rev. D* **81**, 031104 (2010).
  - [13] R. Mizuk *et al.* (Belle Collaboration), Evidence for the  $\eta_b(2S)$  and Observation of  $h_b(1P) \rightarrow \eta_b(1S)\gamma$  and  $h_b(2P) \rightarrow \eta_b(1S)\gamma$ , *Phys. Rev. Lett.* **109**, 232002 (2012).
  - [14] U. Tamponi *et al.* (Belle Collaboration), First Observation of the Hadronic Transition  $\Upsilon(4S) \rightarrow \eta h_b(1P)$  and New Measurement of the  $h_b(1P)$  and  $\eta_b(1S)$  Parameters, *Phys. Rev. Lett.* **115**, 142001 (2015).
  - [15] J. P. Lees *et al.* (BABAR Collaboration), Study of radiative bottomonium transitions using converted photons, *Phys. Rev. D* **84**, 072002 (2011).
  - [16] S. Dobbs, Z. Metreveli, K. K. Seth, A. Tomaradze and T. Xiao, Observation of  $\eta_b(2S)$  in  $\Upsilon(2S) \rightarrow \gamma\eta_b(2S)$ ,  $\eta_b(2S) \rightarrow$  Hadrons, and Confirmation of  $\eta_b(1S)$ , *Phys. Rev. Lett.* **109**, 082001 (2012).
  - [17] S. Sandilya *et al.* (Belle Collaboration), Search for Bottomonium States in Exclusive Radiative  $\Upsilon(2S)$  Decays, *Phys. Rev. Lett.* **111**, 112001 (2013).
  - [18] J. P. Lees *et al.* (BABAR Collaboration), Evidence for the  $h_b(1P)$  meson in the decay  $\Upsilon(3S) \rightarrow \pi^0 h_b(1P)$ , *Phys. Rev. D* **84**, 091101 (2011).
  - [19] I. Adachi *et al.* (Belle Collaboration), First Observation of the  $P$ -wave Spin-Singlet Bottomonium States  $h_b(1P)$  and  $h_b(2P)$ ,

- Phys. Rev. Lett. **108**, 032001 (2012).
- [20] A. E. Bondar, R. V. Mizuk and M. B. Voloshin, Bottomonium-like states: Physics case for energy scan above the  $B\bar{B}$  threshold at Belle-II, Mod. Phys. Lett. A **32**, 1750025 (2017).
- [21] G. Aad *et al.* (ATLAS Collaboration), Observation of a New  $\chi_b$  State in Radiative Transitions to  $\Upsilon(1S)$  and  $\Upsilon(2S)$  at ATLAS, Phys. Rev. Lett. **108**, 152001 (2012).
- [22] V. M. Abazov *et al.* (D0 Collaboration), Observation of a narrow mass state decaying into  $\Upsilon(1S) + \gamma$  in  $p\bar{p}$  collisions at  $\sqrt{s} = 1.96$  TeV, Phys. Rev. D **86**, 031103 (2012).
- [23] R. Aaij *et al.* (LHCb Collaboration), Study of  $\chi_b$  meson production in pp collisions at  $\sqrt{s} = 7$  and 8 TeV and observation of the decay  $\chi_b(3P) \rightarrow \Upsilon(3S)\gamma$ , Eur. Phys. J. C **74**, 3092 (2014).
- [24] R. Aaij *et al.* (LHCb Collaboration), Measurement of the  $\chi_b(3P)$  mass and of the relative rate of  $\chi_{b1}(1P)$  and  $\chi_{b2}(1P)$  production, J. High Energy Phys. **1410** (2014) 088.
- [25] R. Mizuk *et al.* (Belle Collaboration), Observation of a new structure near 10.75 GeV in the energy dependence of the  $e^+e^- \rightarrow \Upsilon(nS)\pi^+\pi^-$  ( $n = 1, 2, 3$ ) cross sections, J. High Energy Phys. **1910** (2019) 220.
- [26] E. Kou *et al.* (Belle-II Collaboration), The Belle II Physics Book, Prog. Theor. Exp. Phys. **2019**, 123C01 (2019).
- [27] W. J. Deng, H. Liu, L. C. Gui and X. H. Zhong, Spectrum and electromagnetic transitions of bottomonium, Phys. Rev. D **95**, 074002 (2017).
- [28] B. Q. Li and K. T. Chao, Bottomonium spectrum with screened potential, Commun. Theor. Phys. **52**, 653 (2009).
- [29] N. R. Soni, B. R. Joshi, R. P. Shah, H. R. Chauhan and J. N. Pandya,  $Q\bar{Q}$  ( $Q \in \{b, c\}$ ) spectroscopy using the Cornell potential, Eur. Phys. J. C **78**, 592 (2018).
- [30] M. Shah, A. Parmar and P. C. Vinodkumar, Leptonic and Digamma decay properties of  $S$ -wave quarkonia states, Phys. Rev. D **86**, 034015 (2012).
- [31] S. N. Gupta, S. F. Radford and W. W. Repko, Semirelativistic potential model for heavy quarkonia, Phys. Rev. D **34**, 201 (1986).
- [32] A. M. Badalian, A. I. Veselov and B. L. G. Bakker, Restriction on the strong coupling constant in the IR region from the 1D-1P splitting in bottomonium, Phys. Rev. D **70**, 016007 (2004).
- [33] S. Godfrey and N. Isgur, Mesons in a relativized quark model with chromodynamics, Phys. Rev. D **32**, 189 (1985).
- [34] S. Godfrey and K. Moats, Bottomonium mesons and strategies for their observation, Phys. Rev. D **92**, 054034 (2015).
- [35] J. Z. Wang, Z. F. Sun, X. Liu and T. Matsuki, Higher bottomonium zoo, Eur. Phys. J. C **78**, 915 (2018).
- [36] D. Ebert, R. N. Faustov and V. O. Galkin, Spectroscopy and Regge trajectories of heavy quarkonia and  $B_c$  mesons, Eur. Phys. J. C **71**, 1825 (2011).
- [37] M. Bhat, A. P. Monteiro and K. B. Vijaya Kumar, Properties of bottomonium in a relativistic quark model, arXiv:1702.06774.
- [38] C. S. Fischer, S. Kubrak and R. Williams, Spectra of heavy mesons in the Bethe-Salpeter approach, Eur. Phys. J. A **51**, 10 (2015).
- [39] E. van Beveren, G. Rupp, T. A. Rijken and C. Dullemond, Radial spectra and hadronic decay widths of light and heavy mesons, Phys. Rev. D **27**, 1527 (1983).
- [40] N. A. Tornqvist, The  $\Upsilon(5S)$  Mass and  $e^+e^- \rightarrow B\bar{B}, B\bar{B}^*, B^*\bar{B}^*$  as Sensitive Tests of the Unitarized Quark Model, Phys. Rev. Lett. **53**, 878 (1984).
- [41] J. F. Liu and G. J. Ding, Bottomonium spectrum with coupled-channel effects, Eur. Phys. J. C **72**, 1981 (2012).
- [42] Y. Lu, M. N. Anwar and B. S. Zou, Coupled-channel effects for the bottomonium with realistic wave functions, Phys. Rev. D **94**, 034021 (2016).
- [43] Z. G. Wang, Analysis of the heavy quarkonium states  $h_c$  and  $h_b$  with QCD sum rules, Eur. Phys. J. C **73**, 2533 (2013).
- [44] K. Azizi and J. Y. Süngü, On the mass and decay constant of the P-wave ground and radially excited  $h_c$  and  $h_b$  axial-vector mesons, J. Phys. G **46**, 035001 (2019).
- [45] D. M. Li, B. Ma, Y. X. Li, Q. K. Yao and H. Yu, Meson spectrum in Regge phenomenology, Eur. Phys. J. C **37**, 323 (2004).
- [46] S. S. Gershtein, A. K. Likhoded and A. V. Luchinsky, Systematics of heavy quarkonia from Regge trajectories on  $(n, M^2)$  and  $(M^2, J)$  planes, Phys. Rev. D **74**, 016002 (2006).
- [47] K. W. Wei and X. H. Guo, Mass spectra of doubly heavy mesons in Regge phenomenology, Phys. Rev. D **81**, 076005 (2010).
- [48] A. M. Badalian and B. L. G. Bakker, Radial and orbital Regge trajectories in heavy quarkonia, Phys. Rev. D **100**, 054036 (2019).
- [49] J. O. Daldrop *et al.* (HPQCD Collaboration), Prediction of the Bottomonium D-Wave Spectrum from Full Lattice QCD, Phys. Rev. Lett. **108**, 102003 (2012).
- [50] R. Lewis and R. M. Woloshyn, Higher angular momentum states of bottomonium in lattice nonrelativistic QCD, Phys. Rev. D **85**, 114509 (2012).
- [51] M. Wurtz, R. Lewis and R. M. Woloshyn, Free-form smearing for bottomonium and  $B$  meson spectroscopy, Phys. Rev. D **92**, 054504 (2015).
- [52] Y. Kiyo and Y. Sumino, Perturbative heavy quarkonium spectrum at next-to-next-to-next-to-leading order, Phys. Lett. B **730**, 76 (2014).
- [53] N. Brambilla, G. M. Prosperi and A. Vairo, Three body relativistic flux tube model from QCD Wilson loop approach, Phys. Lett. B **362**, 113 (1995).
- [54] B. Chen, K. W. Wei and A. Zhang, Assignments of  $\Lambda_Q$  and  $\Xi_Q$  baryons in the heavy quark-light diquark picture, Eur. Phys. J. A **51**, 82 (2015).
- [55] R. Aaij *et al.* (LHCb Collaboration), Study of the  $D^0 p$  amplitude in  $\Lambda_b^0 \rightarrow D^0 p \pi^-$  decays, J. High Energy Phys. **1705** (2017) 030.
- [56] R. Aaij *et al.* (LHCb Collaboration), Observation of New Resonances in the  $\Lambda_b^0 \pi^+ \pi^-$  System, Phys. Rev. Lett. **123**, 152001 (2019).
- [57] D. LaCourse and M. G. Olsson, The string potential model: Spinless quarks, Phys. Rev. D **39**, 2751 (1989).
- [58] T. J. Allen and M. G. Olsson, Reduction of the QCD string to a time component vector potential, Phys. Rev. D **68**, 054022 (2003).
- [59] F. Buisseret and C. Semay, Auxiliary fields and the flux tube model, Phys. Rev. D **70**, 077501 (2004).
- [60] Y. Nambu, Quark model and the factorization of the Veneziano amplitude, in *Proceedings of the International Conference On Symmetries and Quark Models* (Gordon and Breach, New York, 1970), p. 269.
- [61] L. Susskind, Dual-symmetric theory of hadrons.–I, Nuovo Cimento A **69**, 457 (1970).
- [62] T. Goto, Relativistic quantum mechanics of one-dimensional mechanical continuum and subsidiary condition of dual resonance model, Prog. Theor. Phys. **46**, 1560 (1971).
- [63] C. Olson, M. G. Olsson and K. Williams, QCD: Relativistic flux tubes and potential models, Phys. Rev. D **45**, 4307 (1992).
- [64] M. G. Olsson and K. Williams, QCD and the relativistic flux tube with fermionic ends, Phys. Rev. D **48**, 417 (1993).
- [65] C. Olson, M. G. Olsson and D. LaCourse, The Quantized relativistic flux tube, Phys. Rev. D **49**, 4675 (1994).
- [66] M. G. Olsson and S. Veseli, Asymmetric flux tube, Phys. Rev. D **51**, 3578 (1995).

- [67] M. G. Olsson, S. Veseli and K. Williams, Fermion confinement by a relativistic flux tube, *Phys. Rev. D* **53**, 4006 (1996).
- [68] F. Buisseret and C. Semay, Lagrange mesh, relativistic flux tube, and rotating string, *Phys. Rev. E* **71**, 026705 (2005).
- [69] F. Buisseret and C. Semay, Relativistic corrections for two- and three-body flux tube model, *Phys. Rev. D* **76**, 017501 (2007).
- [70] F. Buisseret and C. Semay, Quark self-energy and relativistic flux tube model, *Phys. Rev. D* **71**, 034019 (2005).
- [71] N. Brambilla and G. M. Prosperi, Flux-tube model, quark-antiquark potential, and Bethe-Salpeter kernel, *Phys. Rev. D* **47**, 2107 (1993).
- [72] H. Y. Shan and A. Zhang,  $D$  and  $D_s$  in mass loaded flux tube, *Chin. Phys. C* **34**, 16 (2010).
- [73] B. Chen, D. X. Wang and A. Zhang, Interpretation of  $D_{sJ}(2632)^+$ ,  $D_{s1}(2700)^+$ ,  $D_{sJ}^*(2860)^+$  and  $D_{sJ}(3040)^+$ , *Phys. Rev. D* **80**, 071502 (2009).
- [74] D. Jia and W. C. Dong, Regge-like spectra of excited singly heavy mesons, *Eur. Phys. J. Plus* **134**, 123 (2019).
- [75] T. J. Burns, F. Piccinini, A. D. Polosa and C. Sabelli, The  $2^{++}$  assignment for the  $X(3872)$ , *Phys. Rev. D* **82**, 074003 (2010).
- [76] D. Jia, W. N. Liu and A. Hosaka, Regge Behaviors in Low-lying Singly Charmed and Bottom Baryons, arXiv:1907.04958.
- [77] M. Iwasaki, S. I. Nawa, T. Sanada and F. Takagi, Flux tube model for glueballs, *Phys. Rev. D* **68**, 074007 (2003).
- [78] F. Buisseret, Meson and glueball spectra with the relativistic flux tube model, *Phys. Rev. C* **76**, 025206 (2007).
- [79] H. Nandan and A. Ranjan, Regge trajectories of exotic hadrons in the flux tube model, *Int. J. Mod. Phys. A* **31**, 1650007 (2016).
- [80] M. Iwasaki and F. Takagi, Mass spectra and decay widths of hadrons in the relativistic string model, *Phys. Rev. D* **59**, 094024 (1999).
- [81] T. J. Burns, How the small hyperfine splitting of  $P$ -wave mesons evades large loop corrections, *Phys. Rev. D* **84**, 034021 (2011).
- [82] T. Barnes, S. Godfrey and E. S. Swanson, Higher charmonia, *Phys. Rev. D* **72**, 054026 (2005).
- [83] J. Vijande, F. Fernandez and A. Valcarce, Constituent quark model study of the meson spectra, *J. Phys. G* **31**, 481 (2005).
- [84] P. Bicudo, M. Cardoso, N. Cardoso and M. Wagner, Bottomonium resonances with  $I = 0$  from lattice QCD correlation functions with static and light quarks, arXiv:1910.04827.
- [85] A. M. Badalian, B. L. G. Bakker and I. V. Danilkin, On the possibility to observe higher  $n^3D_1$  bottomonium states in the  $e^+e^-$  processes, *Phys. Rev. D* **79**, 037505 (2009).
- [86] J. Ferretti and E. Santopinto, Threshold corrections of  $\chi_c(2P)$  and  $\chi_b(3P)$  states and  $J/\psi\rho$  and  $J/\psi\omega$  transitions of the  $\chi(3872)$  in a coupled-channel model, *Phys. Lett. B* **789**, 550 (2019).
- [87] E. van Beveren and G. Rupp, Observation of the  $\Upsilon(2^3D_1)$  and indication of the  $\Upsilon(1^3D_1)$ , arXiv:1009.4097.
- [88] B. Aubert *et al.* (BABAR Collaboration), Study of hadronic transitions between  $\Upsilon$  states and observation of  $\Upsilon(4S) \rightarrow \eta\Upsilon(1S)$  decay, *Phys. Rev. D* **78**, 112002 (2008).
- [89] Z. G. Wang, Vector hidden-bottom tetraquark candidate:  $Y(10750)$ , *Chin. Phys. C* **43**, 123102 (2019).
- [90] Q. Li, M. S. Liu, Q. F. Lü, L. C. Gui and X. H. Zhong, Canonical interpretation of  $Y(10750)$  and  $\Upsilon(10860)$  in the  $\Upsilon$  family, *Eur. Phys. J. C* **80**, 59 (2020).
- [91] E. Eichten, K. Gottfried, T. Kinoshita, J. B. Kogut, K. D. Lane and T. M. Yan, Spectrum of Charmed Quark-Antiquark Bound States, *Phys. Rev. Lett.* **34**, 369 (1975), Erratum, *Phys. Rev. Lett.* **36**, 1276 (1976).
- [92] E. Eichten, K. Gottfried, T. Kinoshita, K. D. Lane and T. M. Yan, Charmonium: The model, *Phys. Rev. D* **17**, 3090 (1978), Erratum, *Phys. Rev. D* **21**, 313 (1980).
- [93] S. K. Bose, A. Jabs and H. J. W. Muller-Kirsten, Comments on quark-confinement potentials, *Phys. Rev. D* **13**, 1489 (1976).
- [94] C. Quigg and J. L. Rosner, Quantum Mechanics with Applications to Quarkonium, *Phys. Rept.* **56**, 167 (1979).
- [95] G. Karl and V. A. Novikov, Variational estimates for excited states, *Phys. Rev. D* **51**, 5069 (1995), Erratum, *Phys. Rev. D* **55**, 4496 (1997).
- [96] U. Sukhatme and T. Imbo, Shifted  $1/N$  expansions for energy eigenvalues of the Schrödinger equation, *Phys. Rev. D* **28**, 418 (1983).
- [97] J. M. Richard, The nonrelativistic three-body problem for baryons, *Phys. Rep.* **212**, 1 (1992).